Inorganic Chemistry

Article

pubs.acs.org/IC

# Novel Antitumor Agent, Trilacunary Keggin-Type Tungstobismuthate, Inhibits Proliferation and Induces Apoptosis in Human Gastric Cancer SGC-7901 Cells

Lu Wang,[†,‡] Bai-Bin Zhou,*[,†] Kai Yu,[†] Zhan-Hua Su,[†] Song Gao,[†] Li-Li Chu,[†] Jia-Ren Liu,*[,§] and Guo-Yu Yang*[,∥]

[†]Key Laboratory of Synthesis of Functional Materials and Green Catalysis Colleges of Heilongjiang Province, Department of Chemical Engineering, Harbin Normal University, Harbin, Heilongjiang 150025, People's Republic of China

[‡]Department of Biochemical Engineering, Harbin Institute of Technology, Harbin, Heilongjiang 150090, People's Republic of China

[§]Harvard Medical School (CHB), 300 Longwood Ave, Boston, Massachusetts 02115-5737, United States

[∥]State Key Laboratory of Structural Chemistry, Fujian Institute of Research on the Structure of Matter, Chinese Academy of Sciences, Fuzhou, Fujian 350002, People's Republic of China

Supporting Information

**ABSTRACT:** A new one-dimensional chain-like compound of tungstobismuthate, $[(W(OH)_2)_2\ (Mn(H_2O)_3)_2(Na_3(H_2O)_{14})(BiW_9O_{33})_2](Himi)_2{\cdot}16H_2O$ (**1**) (imi = iminazole), has been synthesized in aqueous solution. The structure of **1** was identified by elemental analysis, IR, thermogravimetry (TG), X-ray photoelectron spectroscopy (XPS), $^{183}$W-NMR, and single crystal X-ray diffraction. To investigate the inhibitory effect of **1** on human gastric adenocarcinoma SGC-7901 cells, cell proliferation and apoptosis initiation were examined by MTT assay (MTT = 3-[4,5-dimethylthiazol-2-yl]-2,5-diphenyl tetrazoliumbromide), flow cytometry, nuclear staining, transmission electron microscopy, single cell gel electrophoresis, DNA fragmentation, and Western blotting. The results showed that **1** inhibited cell proliferation and induced apoptosis in SGC-7901 cells in dose-dependent manner. In addition, **1** also decreased the expression of bcl-2 protein and nuclear factor-$\kappa$B p65 protein in SGC-7901 cells. And expression of bcl-2 protein exhibits a decreasing trend with increase of concentration of **1**. Thus, **1** possessed a potential antitumor activity in SGC-7901 cells. This suggests that polyoxotungstates will provide a promising and novel antitumor agent in prevention and treatment of gastric adenocarcinoma.

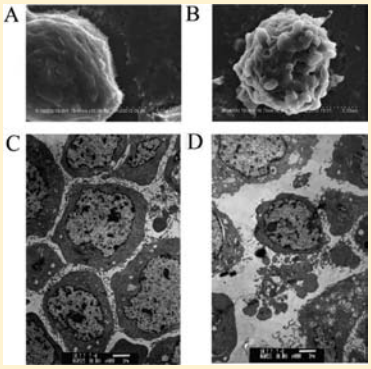


## INTRODUCTION

Interest in polyoxometalates (POMs) has traditionally been focused on their unique structure and alterable properties including design and synthesis of new POMs as well as their consequent diversified applications in catalysis, photoelectric chemistry, and magnetism, and so forth.[1−3] POMs have advantageous structural characteristics and chemical properties in drug synthesis.[4,5] POMs have a strong effect on the target recognition of biological macromolecules following their properties such as polarity, redox potentials, surface charge distribution (high negative), shape, nucleophilicity, and acidity. In addition, POMs also regulate the molecular biological effects and enhance the recognition of target secondary structure of biological macromolecules through covalent linkages with organic groups. Therefore, the bioactivities of POMs in the biosystem are still unclear.

Cancer has been one of the serious public health problems which has threatened human health in the world. Chemotherapeutics has become an important method in the treatment of tumors. Therefore, to find a potent antitumor drug with low-toxicity has become the priority in the chemotherapeutic treatment of tumors.[6−10] Up to 1990s, many studies have focused on the antiviral,[11−18] antibacterial,[19−23] and antitumoral[24−47] effect of POMs. In 1973, Jasmin et al. found that $[NH_4]_{17}Na[NaSb_9W_{21}O_{86}]{\cdot}14H_2O$ (HPA-23) could inhibit virus-induced tumor;[48] In 1980, Jozsef first used $(NH_4)_6[Mo_7O_{24}]{\cdot}6H_2O$ in a patented prescription against cancer. In 1988, Yamase found the antitumor activity of $(NH_3Pri)_6[Mo_7O_{24}]\ 3H_2O$ (PM-8).[24] In 1992, $Na[IMo_6O_{24}]$ was applied as an anticolon cancer drug to clinical patients.[42] In 2004, Wang reported the antitumor activity of heteropolytungstates and polyoxovanadate modified by organic amine in vitro.[49,50] In 2008, Prudent reported the identification of POMs as nanomolar noncompetitive inhibitors of protein kinase CK2.[35] In 2010, Compain showed the activity of tetra- to dodeca-nuclear oxomolybdate complexes with functionalized bisphosphonate ligands in killing tumor cells.[43] In addition, Ogata reported the antitumor effect of $[Me_3NH]_6[H_2Mo_{12}O_{28}(OH)_{12}(MoO_3)_4]{\cdot}2H_2O$(PM-17) on

**Received:** January 4, 2013
**Published:** April 10, 2013

   dx.doi.org/10.1021/ic400019r | Inorg. Chem. 2013, 52, 5119−5127

cell apoptosis both in vitro and in vivo models.[34] Thus, many studies have focused on apoptosis induced by POMs which may be one of the mechanisms of inhibiting tumor cell proliferation.

Because POMs are simultaneously $\pi$-donor/acceptor ligands, the lacunary polytungstates can provide polydentate coordination sites for most metal cations. As inorganic polydentate ligands, polytungstates have wide applications to bond to other transition metals.[51−55] For example, bismuth compounds are used for the treatment of gastrointestinal disorders. Bismuth complexes have also been shown to exhibit medical activity.[56−59] For example, Li reported the antitumor and antibacterial activity of bismuth complexes containing heterocyclic thiosemicarbazones.[60−63] In addition, iminazole (imi) and its derivates are one of the most commonly used drug ligands, which not only possess a variety of the coordination, but also have the medicinal perspective.[64,65] However, it is not yet reported in how to combine and use them organically to form new compounds with antitumor activities. Thus, the objectives of this study were to determine a one-dimensional (1-D) chainlike trilacunary Keggin-type tungstobismuthates modified with imi, $[(W(OH)_2)_2(Mn(H_2O)_3)_2(Na_3(H_2O)_{14})(BiW_9O_{33})_2]$ $(Him)_2{\cdot}16H_2O$ (**1**) which (1) synthesized the method; (2) identified the structural characteristics by elemental analysis, IR, thermogravimetry (TG), and single-crystal X-ray diffraction; and (3) inhibited proliferation and induced apoptosis in human gastric adenocarcinoma SGC-7901 cells.

## MATERIALS AND EXPERIMENTS

**Chemicals, Reagents, and Instruments.** Ethylene diamine tetra acetic acid disodium salt (EDTA), MTT (3-[4,5-dimethylthiazol-2-yl]-2,5-diphenyl tetrazoliumbromide) and dimethylsulfoxide were purchased from Sigma Chemicals Co. (St. Louis, MO). Rabbit polyclonal antibodies for $\beta$-actin (sc-1616-R), Bcl-2 (sc-492), and NF-$\kappa$B p65 (sc-372) were bought from Santa Cruz Biotechnology (Santa Cruz, CA, U.S.A.). Goat antirabbit (w3960) and antimouse (w3950) secondary antibodies were purchased from Promega.

Elemental analyses (C, H, and N) were performed on a Perkin-Elmer 2400 CHN elemental analyzer. Na, Bi, W, and Mn analyses were performed on a PLASMA-SPEC (I) ICP atomic emission spectrometer. The $^{183}$W-NMR spectra were recorded on a Bruker DRX 500 instruments at 16.67 MHz using $D_2O$ as a solvent in 10-mm tubes. As references (external standards) we used aqueous solutions of 1 M $Na_2WO_4$. X-ray photoelectron spectroscopy (XPS) analyses were performed on a VG ESCALAB MK II spectrometer with a Mg K$\alpha$ (1253.6 eV) achromatic X-ray source. The vacuum inside the analysis chamber was maintained at $6.2 \times 10^{-6}$ Pa during analysis. IR spectrum was recorded in the range 400−4000 $cm^{-1}$ on an Alpha Centaurt FT/IR Spectrophotometer using KBr pellets. Diffuse reflectance UV−vis spectra ($BaSO_4$ pellets) were obtained with a Varian Cary 500 UV−vis NIR spectrometer. TG analyses were performed on a Perkin−Elmer TGA7 instrument in flowing $N_2$ with a heating rate of 10 °C·$min^{-1}$. Electrochemical measurements were performed with a CHI660 electrochemical workstation. A conventional three-electrode system was used. The working electrode was a glassy carbon electrode. Platinum gauze was used as a counter electrode, and Ag/AgCl was used as reference electrode. The morphologies and sizes of the products were characterized by using Hitachi S-4800 field emission scanning electron microscopy (FE-SEM) and a TECNAI $G^2$ F20 S-TWIN high-resolution transmission electron microscope (TEM).

**Syntheses of POMs.** A mixture of $Na_2WO_4{\cdot}2H_2O$ (1.55 g), $Bi(NO_3)_3{\cdot}5H_2O$ (0.2425 g), imi (0.069 g), and $MnCl_2{\cdot}6H_2O$ (0.13 g) in a molar ratio of 4.70:0.50:1.00:0.70 was dissolved in $H_2O$ (40 mL) and stirred for 2 h at 80 °C. Then, pH value of the resulting mixture was adjusted to 6.8 with 1 M NaOH solution. During this period, the pH value of the solution was adjusted to 6.8 with a solution of NaOH (0.25 mol/L). The final mixture was filtered and cooled at room temperature. The isolated yellow crystals were collected by filtration a few days later, and dried at room temperature. The rate of yield was 56% (based on Bi). $[(W(OH)_2)_2(Mn(H_2O)_3)_2(Na_3(H_2O)_{14})(BiW_9O_{33})_2](Him)_2{\cdot}16H_2O$ (**1**) (6175.59) was calculated: C 1.18, H 1.31, N 0.92, Mn 1.80, W 60.15, Bi 6.84, Na 1.51; found C 1.14, H 1.27, N 0.91, Mn 1.87, W 60.29, Bi 6.77, Na 1.42. IR (KBr pellet, $cm^{-1}$): 3395 (br), 3137 (br), 1630 (s), 1425 (s), 1169 (m), 941 (s), 821 (s), 760 (s).

**Determination of Crystal Structure 1.** crystal data were collected on a Bruker Smart CCD diffractometer with Mo K$\alpha$ radiation ($\lambda$ = 0.71073 Å) at 273 K. Semiempirical absorption correction was applied. The structures of **1** were solved by direct methods and refined on $F^2$ by the full-matrix least-squares using the SHELXTL-97 crystallographic software.[66,67] Anisotropic thermal parameters were refined to all of the non-hydrogen atoms. The hydrogen atoms were held in calculated positions on carbon atoms and nitrogen atoms, and the hydrogen atoms on oxygen atoms directly included in the final molecular formula on water molecules and protonated oxygen atoms. The crystallographic data and structure refinement were provided in Supporting Information, Table S1. Selected bond lengths and angles were listed in Supporting Information, Table S2. CCDC-730763 contains the supplementary crystallographic data for this paper. These data can be obtained from the Cambridge Crystallographic Data Centre via ww.ccdc.cam.ac.uk/data_request/cif.

**Cell Culture.** Human gastric adenocarcinoma SGC-7901 cells were obtained from the Cancer Institute of Chinese Academy of Medical Science (Beijing, China). The **1** solution was adjusted by dissolution in 10% fetal bovine serum (FBS) RPMI 1640 medium (GIBCO). SGC-7901 cells were maintained in FBS RPMI 1640 medium supplemented with 10% FBS, 100 IU/mL penicillin, 100 $\mu$g/mL streptomycin, and 2 mmol/L glutamine, at 37 °C in a 5% $CO_2$ atmosphere. The medium was changed every 3 days, and cells were passaged with 0.25% trypsin. Cells were plated at a density of $1 \times 10^6$ cells per 100 mm culture dish and allowed to grow to approximately 70% confluence before experimentation.

**Cell Proliferation.** The effect of **1** on cell viability was determined in SGC-7901 cells as described in a previous study.[68] Briefly, cells were seeded in a 96-well microtiter plate (Nunc, Wiesbaden, Germany) at $1.0 \times 10^4$ cells per well. After 24 h of incubation, the cells were treated with 200 $\mu$L of medium containing various concentrations (50, 100, 200, 300, and 400 $\mu$mol/L) of **1** for 24 h. For each concentration, five replicates were employed. Twenty microliters of 5 mg/mL MTT solution was added to each well, and cells continued to be incubated for 4 h at 37 °C. After careful removal of the medium, 200 $\mu$L of dimethyl sulfoxide (DMSO) was added to each well, and the plate was then shaken for about 10 min until the crystals were solubilized. Absorbance was then measured at 490 nm in a microplate reader (Elx800 Universal Microplate Reader, Bio-Tek Instruments, U.S.A.). 5-Fluorouracil (5-FU) and cisplatin (cis-DDP) were used as positive controls in this study. To compare to other derivatives, tungstates ($Na_2WO_4{\cdot}2H_2O$), bismuthates ($Bi(NO_3)_3{\cdot}5H_2O$), manganese ($MnCl_2{\cdot}6H_2O$), and imi were also used in this study. The curves of cell viability were drawn by comparing the control group. The inhibitory rate was calculated using the following equation: inhibitory rate (%) = $(OD_{control} - OD_{treatment})/OD_{control} \times 100\%$.

**Morphological Observation.** Apoptosis and necrosis were also determined morphologically using staining with acridine orange (10 mg/mL)/ethidium bromide (10 mg/mL) (AO/EB) as described in a previous study.[69] After treatments, cells were washed and adjusted at a density of $1 \times 10^6$ cells/mL in PBS. Acridine orange/ethidium bromide solution (1:1, v/v) was added to the cell suspension in a final concentration of 100 $\mu$g/mL. The cellular morphology was evaluated by fluorescence microscopy (Olympus IX70, Japan).

**TEM and SEM.** For transmission electron microscopy (TEM), SGC-7901 cells were treated with 200 $\mu$mol/L **1** for 24 h. The cells were harvested and fixed with 2.5% glutaraldehyde dissolved in 0.1 mol/L sodium cacodylate buffer (pH 7.3) for 24 h, followed by 1%


dx.doi.org/10.1021/ic400019r | Inorg. Chem. 2013, 52, 5119−5127

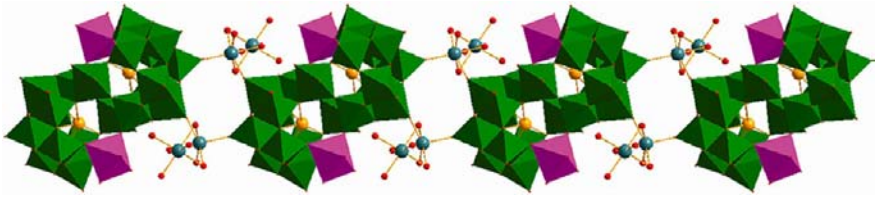

**Figure 1.** 1-D chain of **1** was made by sandwiched POM units and [$Na_2$] linkers (green octahedra, W; purple octahedra, Mn; yellow ball, Bi; blue ball, Na).

osmium tetroxide fixation for 90 min at the room temperature, dehydrated in an acetone series (30−100%) and finally embedded in Epon. Ultrathin sections were stained with uranyl acetate and lead citrate and observed in a transmission electron microscope.[70]

SGC-7901 cancer cells were grown on 20 $mm^2$ coverslips in a 6-well microtiter plate (Nunc, Wiesbaden, Germany) at 1.0 × $10^4$ cells per well. After treatment of 200 $\mu$mol/L **1** for 24 h, cells were fixed with 2.5% glutaraldehyde dissolved in 0.1 mol/L sodium cacodylate for 2 h, postfixed in osmium tetroxide, dehydrated with graded ethylalocoho series, immersed in isoamyl acetate, dried under $CO_2$ critical point, and finally pasted on the stage for specimen. The plating films were examined in a S3400N scanning electron microscope (SEM) (HITACHI, Japan).

**DNA Fragmentation.** DNA fragmentation was determined by extraction of DNA followed by agarose gel electrophoresis. Briefly, cells were treated with **1** for 24 h and then washed twice with PBS, resuspended in the extraction buffer (10 mmol/L Tris, 0.1 mol/L EDTA, 20 $\mu$g/mL trypsin, 5 mg/mL SDS; pH 8.0), and incubated for 1 h at 37 °C. The homogenates were then incubated with 20 mg/mL proteinase K (Merck, Germany) for 3 h at 50 °C. After phenol extraction, DNA was precipitated and dissolved in the TE buffer and electrophoresed on a 1.2% agarose gel. The gel was stained with ethidium bromide (20 $\mu$g/mL) and photographed under ultraviolet.

**Apoptotic Analysis by FCM.** After treatment of **1**, SGC-7901 cells were collected, washed with cool PBS, suspended in 500 $\mu$L of binding buffer (Annexin V$^-$FITC Apoptosis Detection Kit, KeyGEN), mixed with 5 $\mu$L of fluorescein isothiocyanate (FITC)-conjugated annexin V (Annexin V$^-$FITC), and stained with 5 $\mu$L of propidium iodide (PI) (Annexin V$^-$FITC Apoptosis Detection Kit, KeyGEN) for 10 min at 37 °C away from light according to manufacturer's instructions. For each dose, at least 1.0 × $10^5$ cells were analyzed by a flow cytomery. The population of annexin V$^-$PI$^-$ viable cells and annexin V$^+$ cells was evaluated by flow cytometry (BD Biosciences, U.S.A.). The proportions in four phases were estimated using ModFit LT analysis software.

**Western Blotting.** After treatment of **1** for 24 h, total protein from the cells were extracted in the lysis buffer and following a previous study.[69] Total protein (50−80 $\mu$g) were separated in 10% polyacrylamide gels (SDS-PAGE). The gels were transferred to a nitrocellulose membrane. The membrane was blocked in blocking buffer (1% BSA and 0.1% Tween-20 in 20 mmol/L TBS, pH 7.6) for 1 h at 37 °C in a hybridization oven (Amersham, Life Science), then incubated with bcl-2, NF-$\kappa$B p65, or $\beta$-actin primary antibodies in blocking buffer overnight at 4 °C. After washing TBST 3 times, the membranes were incubated with the corresponding IgG HRP conjugate secondary antibody at 37 °C for 1 h. The membrane was washed two times with TBST, and then washed with TBS. The membranes were then incubated with alkaline phosphatase-conjugated IgG. The protein bands detected with the Western Blue Stabilized Substrate for alkaline phosphatase (Promega).

**Statistical Analysis.** Data were expressed as means ± standard deviation (SD). Three independent experiments were performed in this study. Difference was analyzed using the One-Way ANOVA with the Bonferroni post hoc multiple comparisons to assess the difference between independent groups. Data analyses were generated using SPSS for Windows Version 19.0 (SPSS Inc., Chicago, IL). A statistical significance was set at $P < 0.05$, and all $P$ values were unadjusted for multiple comparisons.

## RESULTS AND DISCUSSION

**Structure of 1.** The structure of $[(W(OH)_2)_2(Mn(H_2O)_3)_2(Na_3(H_2O)_{14})(BiW_9O_{33})_2](Him)_2{\cdot}16H_2O$ is shown in Figure 1. A 1-D chain built up of the sandwich anions $[Mn_2(H_2O)_6(W(OH)_2)_2(\beta\text{-B-}BiW_9O_{33})_2]^{6-}$ and the two $Na^+$ ions is shown in the Supporting Information, Figure S1 and S2. In the chain, the coordination geometries of two $Na^+$ ions are octahedral: the bridging one is coordinated by four water ligands and two $\mu_2$-O atoms from two neighboring sandwich-type $[Mn_2(H_2O)_6(W(OH)_2)_2(\beta\text{-B-}BiW_9O_{33})_2]^{6-}$ anions, and further linked a $Na(H_2O)_6^+$ complex group by three bridging water ligands, resulting in an 1-D chain by double W-O-[$Na_2$]-O-W bridges. Additionally, the independent organic imi is just located in the window formed by two sandwich polyanions and two [$Na_2$] linkers (Supporting Information, Figure S1). In the sandwich-type unit, two identical $[B\text{-}\beta\text{-}BiW_9O_{33}]^{9-}$ moieties are linked by two corner-sharing $WO_6$ octahedra and two octahedral $MnO_3(H_2O)_3$ groups to form the krebs-type structure, $[Mn_2(H_2O)_6(W(OH)_2)_2(\beta\text{-}BiW_9O_{33})_2]^{6-}$ (Supporting Information, Figure S2).

As polyanion **1** is diamagnetic we performed $^{183}$W-NMR studies in solution. The room-temperature $^{183}$W-NMR spectra of **1** exhibits 6 peaks at −48.0, −80.1, −105.2, −120.1, −152.6, and −320.1 ppm with intensity ratios 2:2:2:2:1:1 (see Supporting Information, Figure S3). This result indicates that in solution a species with $C_{2h}$ symmetry is present,[71] which is in complete agreement with the solid state structure of **1**. Furthermore, the NMR spectrum does not change even after 2 weeks, indicating the high stability of **1** in aqueous solution.

Bond valence sum (BVS) calculations[72] confirm that all Bi and W centers are in the oxidation states of +3 and +6, respectively. The Mn and Na cations in compound **1** are all in the +2 and +1 oxidation states, respectively. In addition, BVS calculations for the O toms linked to the W centers (O1, O2) present the hydroxyl ligands (1.18−1.25) and the water molecules linked to the Mn and Na centers (0.22 to 0.34). Moreover, three extra protons should be added to isolated imi molecules of compounds **1** for the charge balance.

**XPS Spectroscopy.** The oxidation states of W and Mn are further confirmed by XPS spectra, which were carried out in the energy region of $W4f_{7/2}$, $W4f_{5/2}$, $Mn2p_{1/2}$, and $Mn2p_{3/2}$ respectively (Supporting Information, Figure S4). The XPS spectra give two peaks at 34.8 and 37.2 eV which are attributed to $W^{6+}$ ions. The peak at 640.8 and 654.1 eV are ascribed to $Mn^{2+}$ ions.[73] The oxidation states of them are in accordance with the valence bond calculations.

**IR Spectroscopy.** The IR spectra exhibited prominent characteristic peaks for the sandwich-type structure at 941, 821, and 760 $cm^{-1}$, which can be ascribed to the (W═$O_d$), (W−$O_b$−W), and (W−$O_c$−W) vibrations of the polyoxoanion cluster. The characteristic peaks concerned with coordinated imi ligands are at 1425(w) and 1169(m)/cm. The strong peak


dx.doi.org/10.1021/ic400019r | Inorg. Chem. 2013, 52, 5119−5127

at 1630 $cm^{-1}$ can be assigned to isolated solvent water molecules. The peaks at 3137−3395/cm were assigned to the N−H and O−H vibrations (Supporting Information, Figure S5).[74]

**TG Analysis.** The TG curve was presented a two-step weight-loss process (Supporting Information, Figure S6). The first step corresponded to the loss of isolated and coordinated water molecules (calculated weight loss 10.30%; found 10.36%) in the temperature range 39−295 °C. The second step corresponded to the loss of the organic imi ligands (calculated weight loss 2.23%; found 2.15%) between 424 and 556 °C.

**Cyclic Voltammogram Analysis.** The cyclic voltammogram of 1.0 mmol/L **1** was detected in the pH 4 (0.4 mol/L $CH_3COONa$ + $CH_3COOH$) buffer solution (Supporting Information, Figure S7). The compound (vs Ag/AgCl) at a scan rate of 20 mV/s appeared with mean peak potentials [$E_{1/2} = (E_{pa} + E_{pc})/2$] of +831(I−I′) and −437(I−I′) mV. The redox peaks I−I′ and II−II′ corresponded to two consecutive one-electron processes of the W atoms.[75]

**Solution Stability.** The stability of **1** was detected in pH 6.8 (dissolved in water, 50 μmol/L). As shown in Supporting Information, Figure S8, there were two absorption bands at about 210 and 250 nm, which respectively related to Od→M and Ob, Oc→M charge transfer transitions. With the prolonged time of the placed solution, the absorption bands were not obviously displaced. The result showed that **1** was stable for the research on drugs.

**Effect of 1 on Growth of SGC-7901 Cells.** To determine the effect of **1** on cell proliferation, cell viability of SGC-7901 cells was examined by MTT assay. The effects of **1** on the viability of SGC-7901 cells is shown in Figure 2; cell viability of

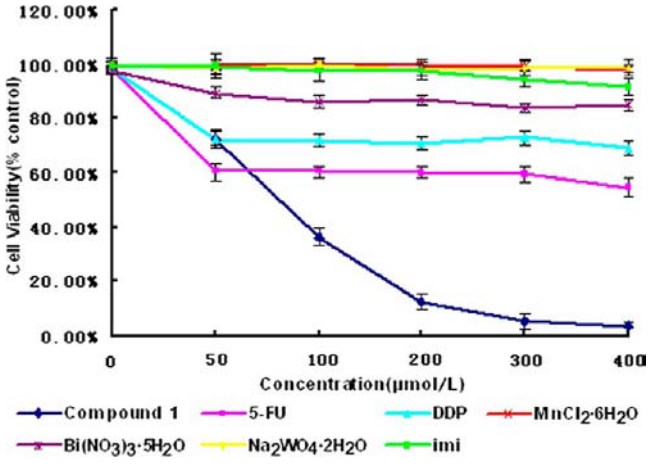


**Figure 2.** Effect of **1** on SGC-7901 cell viability. SGC-7901 cells were exposed to different concentrations of **1** for 24 h, and cell viability was determined by a MTT assay. Cell viability is presented in percentages, and vehicle-treated cells were regarded as 100% viable. Data are presented in mean ± SD ($n$ = 5).

SGC-7901 cells treated with 50, 100, 200, 300, and 400 μmol/L of **1** for 24 h was decreased by 72.6, 36.6, 12.6, 5.5, and 3.8%, respectively, in comparison with the control group. These results showed that **1** inhibited the growth of SGC-7901 cells in a dose-dependent manner ($p < 0.05$ or $p < 0.01$). The 50% inhibitory concentration ($IC_{50}$), the dose of **1** required to inhibit or kill 50% of the cells tested, was 81.0 ± 4.1 μmol/L at 24 h. **1** significantly inhibited the cell proliferation when compared to 5-fluorouracil (5-FU) and cisplatin (cis-DDP) which are commonly clinical chemotherapy drugs. In the meantime, cell viability of tungstates, bismuthates, manganese, and imi in SGC-7901 cells also were tested in this study. The results showed that their cell viability was higher that in a **1** group (Figure 2). Thus, **1** has a potent inhibition of cell proliferation in SCG-7901 cells.

**Effect of 1 on SGC-7901 Cell Morphology.** Apoptosis is a mode of programmed cell death and is an important biological consequence of exposure to extrinsic agents,[76−80] and apoptosis is a complex process regulated by a variety of factors.[81,82] Induction of apoptosis is an important target for cancer therapy.[83,84] In this study, cell morphologic changes were performed in SGC-7901 cells treated with **1**. The cells treated with 200 μmol/L of **1** for 24 h showed a shrinkage, rounding, and fragmentation in contrast with the control cells (Figure 3A). In addition, the induction of apoptosis or necrosis

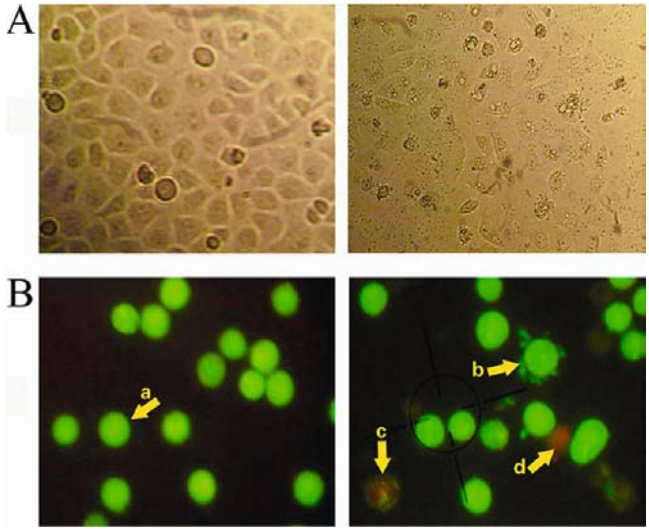


**Figure 3.** Morphological changes of SGC-7901 cells. (A) SGC-7901 cells treated with **1** show shrinkage, rounding, and fragmentation in contrast with untreated cells (original magnification 200×). (B) SGC-7901 cells stained with AO/EB dye. Arrow a shows variable cells (bright green chromatin); arrow b shows early apoptotic cells (bright green highly condensed or fragmented chromatin); arrow c shows late apoptotic cells (bright orange highly condensed or fragmented chromatin); and arrow d shows necrotic cells (bright orange/red chromatin) (original magnification 200×).

was morphologically determined after staining with acridine orange (AO) and ethidium bromide (EB) by fluorescence microscopy (Figure 3B). The results showed that the viable cells were uniformly green, while early apoptotic cells were green with bright green dots in their nuclei as a result of chromatin condensation and nuclear fragmentation. Late apoptotic cells were stained by the EB which incorporated into DNA and therefore showed orange with obvious condensation.

**Effect of 1 on SGC-7901 Cell Ultramicrostructure.** The ultramicrostructure of **1** on SGC-7901 cells was also investigated in this study. As shown in Figure 4, SEM showed the characteristics of apoptosis such as cell membrane blebbing, microvilli disappearance or reduction (Blunt microvillus), and separated apoptotic bodies in the treated cells. Untreated cells showed morphological features including numerous microvillis on its surface with membrane connections. TEM showed a cell shrinkage, increased cellular granularity, the formation of


dx.doi.org/10.1021/ic400019r | Inorg. Chem. 2013, 52, 5119−5127

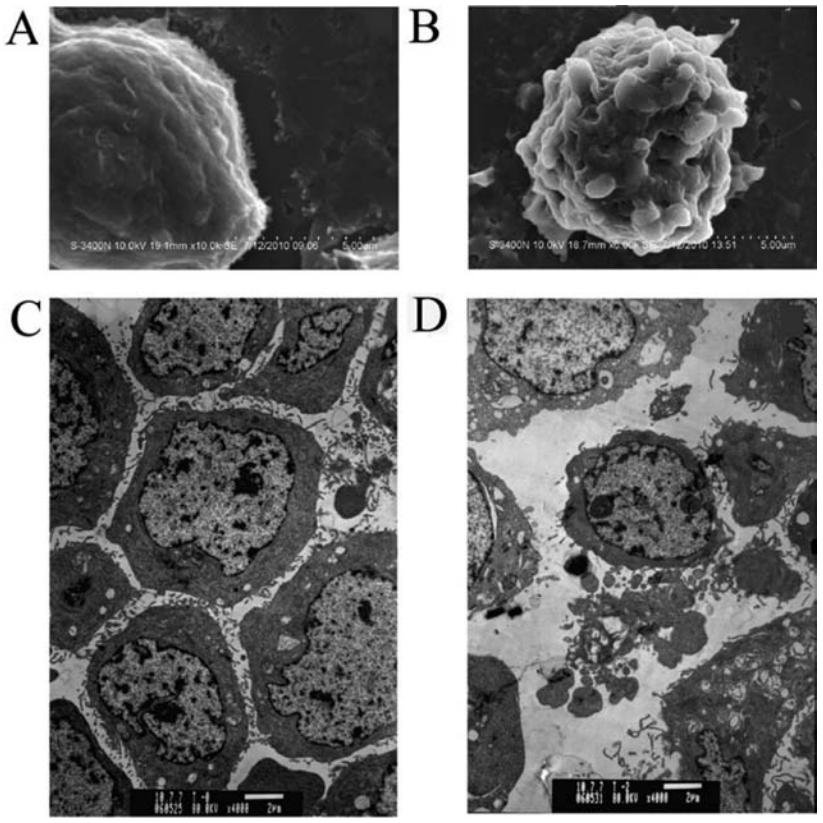


**Figure 4.** Ultrastructural changes in SGC-7901 cells. (A) SEM shows untreated SGC-7901 cell (original magnification 10000×). (B) SEM shows SGC-7901 cells treated with 200 μmol/L of **1** for 24 h. The volume of treated cells decreased, and microvillis on the surface eliminated. Invaginations and globular projections emerged on the surface of apoptotic cells. Bulks of spherule formation splitted from apoptotic cells (original magnification 6000×). (C) TEM shows untreated SGC-7901 cell (original magnification 4000×). (D) TEM shows SGC-7901 cells treated with 200 μmol/L of **1** for 24 h. The treated cells became small and round. The nuclear volume decreased. The chromatin became condensed and diffused in the nuclei. Finally, the cell membrane disappeared and the endocyte spilled (original magnification 4000×).

apoptotic bodies, dilated nuclear membranes, vacuoles in the cytoplasm, and DNA fragmentation in the treated cells (Figures 4 C and D). Untreated cells showed the morphology with randomly distributed organelles and nuclei with finely granular and uniformly dispersed chromatin and a single large electron-dense nucleolus.

**Effect of 1 on SGC-7901 Cell DNA Fragmentation.** The effect of **1** on apoptosis of SGC-7901 cells was further assessed by a DNA fragmentation assay. As shown in Figure 5, a clear DNA ladder was shown in SGC-7901 cells treated with 200 μmol/L of **1** for 24 h. No DNA ladder is found in the control group or in cells supplemented with 50 μmol/L of **1** for 24 h.

**Effect of 1 on SGC-7901 Cell Apoptosis by FCM.** In addition, the annexin V-FITC and PI double-staining techniques were also used to further confirm that **1** induced apoptosis in SGC-7901 cells. Phosphatidylserine expression on the external surface of cells was an early feature of apoptosis changes. Annexin V is a calcium- and phospholipid-binding protein with a high affinity for phosphatidylserine. Annexin V-FITC is sensitive to detect cells in the early phase of apoptosis. This method allows the detection of viable (annexin $V^-$ and $PI^-$), early apoptotic (annexin $V^+$ and $PI^-$), late apoptotic or necrotic cells (annexin $V^+$ and $PI^+$) based on distinct double-staining patterns with a combination of $FITC^-$conjugated annexin V and PI. In this study, **1**-induced apoptosis in SGC-7901 cells was determined by flow-cytometry (FCM). As shown in Figure 6, **1** at dose of 100 μmol/L showed the cell number on the lower and upper right quadrants which

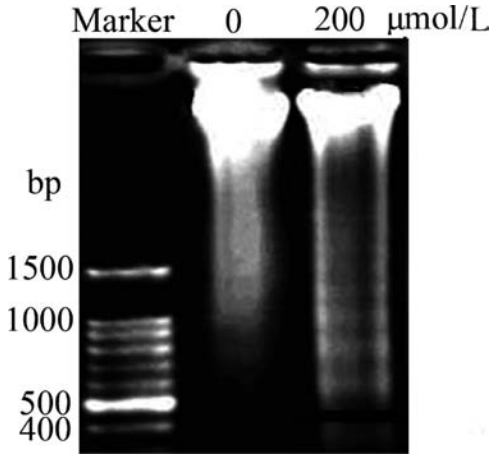


**Figure 5.** Ultrastructural changes in SGC-7901 cells. **1** induced DNA fragmentation in SGC-7901 cells. The cells were treated with 200 μmol/L of **1** for 24 h. DNA was isolated from treated and untreated cells. DNA fragmentation was separated in 1.2% agarose gel. The results showed that **1** induced the DNA ladder in SGC-7901 cells.

represent the percentage of cells in the early stages of apoptosis and in the later stages of cell death, respectively. Thus, these results indicated that **1** could induce late apoptotic and necrotic cells in SGC-7901 cells.

**Western Blot Analysis of Bcl-2 and NF-κB p65 Expression.** The bcl-2 family proteins play critical roles in


dx.doi.org/10.1021/ic400019r | Inorg. Chem. 2013, 52, 5119−5127

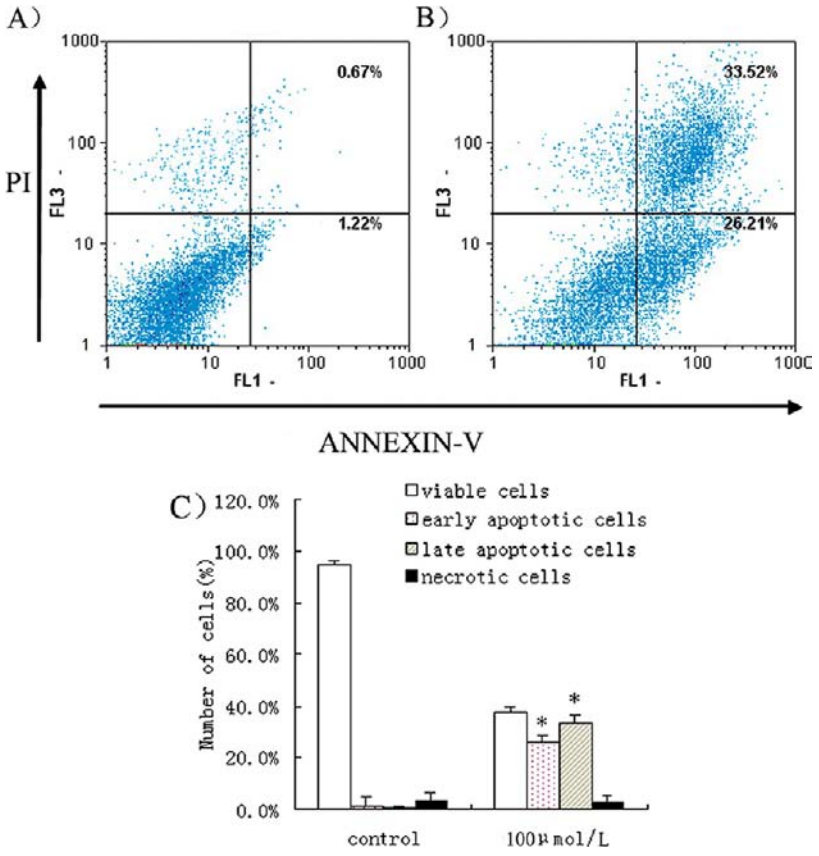


**Figure 6.** Apoptosis determination in SGC-7901 cells by flow cytometry. The cells were exposed to different concentrations of **1** for 24 h. Annexin V-FITC and PI double-staining technique was used to detect cell apoptosis. The fluorescence intensity of PI is plotted on the *y*-axis, and annexin V-FITC on the *x*-axis. A for Control; B for 100 $\mu$mol/L of **1**; and C for statistical results. $P < 0.05$, when compared to the control group.

regulation of cell death processes. The most prominent member of this family that is involved in gastric cancer is bcl-2. The bcl-2 protein is a proto-oncogene that promotes oncogenesis by blocking apoptosis, and the overexpression of bcl-2 could provide a potential mechanism for the growth and subsequent over-accumulation of tumor cells in several cancers.[85−90] Moreover, bcl-2 can block the initiation of apoptosis by inhibiting the apoptosis-inducing release of cytochrome C and apoptosis inhibitory factor into the cytoplasm.[91−93] Bcl-2 proteins can interact with each other and subsequently modulate apoptosis.[85−92] In this study, the expression levels of bcl-2 of SGC-7901 cells treated with 50 $\mu$mol/L of **1** for 24 h did not evidence change in comparison with the negative control. **1** at doses of 100 and 200 $\mu$mol/L significantly decreased expressions of bcl-2 in SGC-7901 cells when compared with the control group. Thus, the results indicated that **1** mediated apoptosis in SGC-7901 cells may depend on the suppression of bcl-2.

To evaluate the possible mechanism of **1** on apoptosis, the expression levels of NF-$\kappa$B p65 protein in SGC-7901 cells were examined by Western blot. As show in Figure 7, the expression of NF-$\kappa$B p65 was down-regulated in the treatment groups when compared to the negative control. This result showed that **1** is involved in the regulation of the pathway of induced cell apoptosis, and may act as signaling regulator to play a role in NF-$\kappa$B signaling transduction in gastric cancer cells. NF-$\kappa$B, a transcriptional activator with potent anti-apoptotic functions has been implicated in resistance to various therapeutic agents in oncogenesis.[94] The NF-$\kappa$B p65 subunit is specifically associated with the regulation of apoptosis, and increased expression of this subunit is important in the pathogenesis of carcinoma.[95,96] Previous studies have shown that the antiproliferative effects of apoptosis agents are correlated with a reduction in NF-$\kappa$B activity.[97−100] NF-$\kappa$B is constitutively activated in gastric adenocarcinoma cancer, where it contributes to the transcriptional activation of a variety of genes involved in proliferation, survival, and chemoresistance of the tumor cells.[95,96] Therefore, our findings showed that **1** decreased NF-$\kappa$B p65 protein expression in SGC-7901 cells. This may be a potential target for antitumor therapy in gastric cancers.

## CONCLUSION

In conclusion, a new synthesized POM, $[(W(OH)_2)_2(Mn(H_2O)_3)_2(Na_4(H_2O)_{14})(BiW_9O_{33})_2]$ $(Him)_2{\cdot}16H_2O$ (**1**), has the biological activity of inhibiting proliferation and inducing apoptosis in human gastric cancer SGC-7901 cells. Induction apoptosis of **1** in human gastric cancer cells was systematically determined and, at least in part, regulation by bcl-2 and NF-$\kappa$B related pathways. These results indicated that POM analogues represent a novel group of selective anticancer agents. However, it is still unclear how **1** regulated bcl-2 or NF-$\kappa$B pathways in POMs-induced cell apoptosis. A further study is needed to explore the possible mechanism. Moreover, we will examine controls with other POM clusters in further scientific studies, in which POMs with the same solubility/charge but with different hetero elements, POMs with different charge/size, and un-"clustered" reagents containing tungstate, bismuth, and so forth will be explored.


dx.doi.org/10.1021/ic400019r | *Inorg. Chem.* 2013, 52, 5119−5127

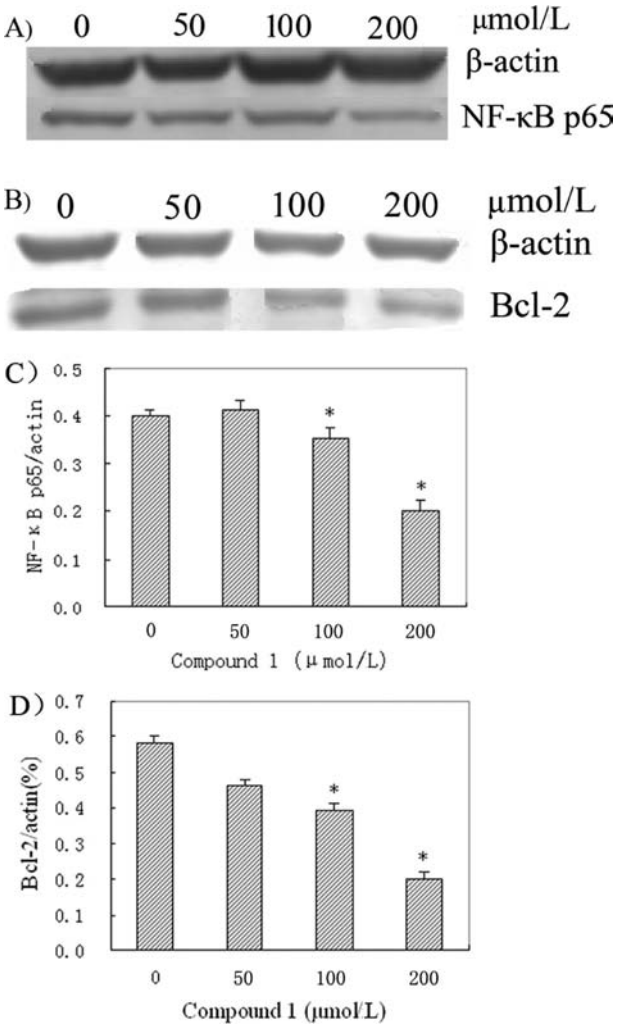


**Figure 7.** Expression of NF-κB p65, bcl-2, and β-actin in SGC-7901 cells. The cells were treated with different concentrations of **1** for 24 h. Protein expression of NF-κB p65, bcl-2, and β-actin in cells was determined by Western blotting. $P < 0.05$, when compared to the control group.

## ■ ASSOCIATED CONTENT

### Ⓢ Supporting Information

X-ray crystallographic data and structure refinement, characteristic IR bands, TG curve, cyclic voltammogram, and stability studies in aqueous media for **1**. This material is available free of charge via the Internet at http://pubs.acs.org..

## ■ AUTHOR INFORMATION


### Corresponding Author

*E-mail: zhou_bai_bin@163.com (B.B.Z.), Jia-Ren.Liu@childrens.harvard.edu (J.R.L.), ygy@fjirsm.ac.cn (G.Y.Y.). Phone: (+86) 0451-88060173 (B.B.Z.).


### Notes

The authors declare no competing financial interest.

## ■ ACKNOWLEDGMENTS


This work was supported the National Natural Science Fund of China (NSF, nos. 20971032 and 21271056), Specialized Research Fund for the Doctoral Program of Higher Education (20122329110001), the Natural Science Foundation of Heilongjiang Province (no. C201037, B201216), the Post-doctoral Science Foundation of Heilongjiang (LBH-Z10292), Doctoral Start-up Foundation of Harbin Normal University (No.KGB201214), the Technological Innovation Team Building Program of the College of Heilongjiang Province (no.2009td04), and the Innovation Team Research Program of Harbin Normal University (no. KJTD200902).


## ■ REFERENCES


(1) Neumann, R. *Inorg. Chem.* **2010**, *49*, 3594.
(2) Fang, X.; Speldrich, M.; Schilder, H.; Cao, R.; O'Halloran, K. P.; Hill, C. L.; Kogerler, P. *Chem. Commun (Cambridge, U.K.).* **2010**, *46*, 2760.
(3) Long, D. L.; Tsunashima, R.; Cronin, L. *Angew. Chem., Int. Ed.* **2010**, *49*, 1736.
(4) Rhule, J. T.; Hill, C. L.; Judd, D. A.; Schinazi, R. F. *Chem. Rev.* **1998**, *98*, 327.
(5) Wu, Q.; Wang, J.; Zhang, L.; Hong, A.; Ren, J. *Angew. Chem.* **2005**, *117*, 4116.
(6) Huang, X.; Zhang, Z.; Jia, L.; Zhao, Y.; Zhang, X.; Wu, K. *Cancer. Lett.* **2010**, *296*, 123.
(7) Ghobrial, I. M.; Witzig, T. E.; Adjei, A. A. *CA Cancer J. Clin.* **2005**, *55*, 178.
(8) Sun, S. Y.; Hail, N.; Lotan, R., Jr. *J. Natl. Cancer. Inst.* **2004**, *96*, 662.
(9) Shukla, S.; Gupta, S. *Nutr. Cancer* **2005**, *53*, 18.
(10) Liu, H. K.; Wang, Q.; Li, Y.; Sun, W. G.; Liu, J. R.; Yang, Y. M.; Xu, W. L.; Sun, X. R.; Chen, B. Q. *J. Nutr. Biochem.* **2010**, *21*, 206.
(11) Raynaud, M.; Chermann, J. C.; Plata, F.; Jasmin, C.; Mathé, G. *C.R. Acad. Sci., Ser. D* **1971**, *272*, 347.
(12) Shigeta, S.; Mori, S.; Watanabe, J.; Baba, M.; Khenkin, A. M.; Hill, C. L.; schinazi, R. F. *Antiviral Chem. Chemother.* **1995**, *6*, 114.
(13) Flutsch, A.; Schroeder, T.; Grutter, M. G.; Patzke, G. R. *Bioorg. Med. Chem. Lett.* **2011**, *21*, 1162.
(14) Take, Y.; Tokutake, Y.; Inouye, Y.; Yoshida, T.; Yamamoto, A.; Yamase, T.; Nakamura, S. *Antiviral Res.* **1991**, *15*, 113.
(15) Shigeta, S.; Mori, S.; Kodama, E.; Kodama, J.; Takahashi, K.; Yamase, T. *Antiviral Res.* **2003**, *58*, 265.
(16) Dan, K.; Yamase, T. *Biomed. Pharmacother.* **2006**, *60*, 169.
(17) Judd, D. A.; Nettles, J. H.; Nevins, N.; Snyder, J. P.; Liotta, D. C.; Tang, J.; Ermolieff, J.; Schinazi, R. F.; Hill, C. L. *J. Am. Chem. Soc.* **2001**, *123*, 886.
(18) Hill, C. L.; Weeks, M. S.; Schinazi, R. F. *J. Med. Chem.* **1990**, *33*, 2767.
(19) Inoue, M.; Suzuki, T.; Fujita, Y.; Oda, M.; Matsumoto, N.; Yamase, T. *J. Inorg. Biochem.* **2006**, *100*, 1225.
(20) Hanaki, H.; Kuwahara-Arai, K.; Boyle-Vavra, S.; Daum, R. S.; Labischinski, H.; Hiramatsu, K. *J. Antimicrob. Chemother.* **1998**, *42*, 199.
(21) Hanaki, H.; Labischinski, H.; Inaba, Y.; Kondo, N.; Murakami, H.; Hiramatsu, K. *J. Antimicrob. Chemother.* **1998**, *42*, 315.
(22) da Silva Coimbra, M. V.; Silva-Carvalho, M. C.; Wisplinghoff, H.; Hall, G. O.; Tallent, S.; Wallace, S.; Edmond, M. B.; Figueiredo, A. M.; Wenzel, R. P. *J. Hosp. Infect.* **2003**, *53*, 103.
(23) Logan, R. P.; Gummett, P. A.; Misiewicz, J. J.; Karim, Q. N.; Walker, M. M.; Baron, J. H. *Lancet* **1991**, *338*, 1249.
(24) Yamase, T.; Fujita, H.; Fukushima, K. *Inorg. Chim. Acta* **1988**, *151*, 15.
(25) Inouye, Y.; Take, Y.; Tokutake, Y.; Yoshida, T.; Yamamoto, A.; Yamase, T.; Nakamura, S. *Chem Pharm. Bull (Tokyo).* **1990**, *38*, 285.
(26) Fukuma, M.; Seto, Y.; Yamase, T. *Antiviral Res.* **1991**, *16*, 327.
(27) Yamase, T. *Mol. Eng.* **1993**, *3*, 241.
(28) Yamase, T.; Fukuda, N.; Tajima, Y. *Biol. Pharm. Bull.* **1996**, *19*, 459.
(29) Fukuda, N.; Yamase, T.; Tajima, Y. *Biol. Pharm. Bull.* **1999**, *22*, 463.
(30) Dan, K.; Miyashita, K.; Seto, Y.; Fujita, H.; Yamase, T. *Pharmacol. Res.* **2002**, *46*, 357.

(31) Ogata, A.; Mitsui, S.; Yanagie, H.; Kasano, H.; Hisa, T.; Yamase, T.; Eriguchi, M. *Biomed. Pharmacother.* **2005**, *59*, 240.
(32) Yanagie, H.; Ogata, A.; Mitsui, S.; Hisa, T.; Yamase, T.; Eriguchi, M. *Biomed. Pharmacother.* **2006**, *60*, 349.
(33) Mitsui, S.; Ogata, A.; Yanagie, H.; Kasano, H.; Hisa, T.; Yamase, T.; Eriguchi, M. *Biomed. Pharmacother.* **2006**, *60*, 353.
(34) Ogata, A.; Yanagie, H.; Ishikawa, E.; Morishita, Y.; Mitsui, S.; Yamashita, A.; Hasumi, K.; Takamoto, S.; Yamase, T.; Eriguchi, M. *Br. J. Cancer.* **2008**, *98*, 399.
(35) Prudent, R.; Sautel, C. F.; Cochet, C. *Biochim. Biophys. Acta* **2010**, *1804*, 493.
(36) Prudent, R.; Moucadel, V.; Laudet, B.; Barette, C.; Lafanechere, L.; Hasenknopf, B.; Li, J.; Bareyt, S.; Lacote, E.; Thorimbert, S.; Malacria, M.; Gouzerh, P.; Cochet, C. *Chem. Biol.* **2008**, *15*, 683.
(37) Wang, X.; Liu, J.; Li, J.; Liu, J. *Inorg. Chem. Commun.* **2010**, *4*, 372.
(38) Wang, X.; Li, F.; Liu, S.; Pope, M. T. *J. Inorg. Biochem.* **2005**, *99*, 452.
(39) Wang, X.; Liu, J.; Pope, M. T. *Dalton. Trans.* **2003**, 957.
(40) Menon, D.; Thomas, R. T.; Narayanan, S.; Maya, S.; Jayakumar, R.; Hussain, F.; Lakshmanan, V. K.; Nair, S. V. *Carbohydr. Polym.* **2011**, *84*, 887.
(41) Zhai, F.; Li, D.; Zhang, C.; Wang, X.; Li, R. *Eur. J. Med. Chem.* **2008**, *43*, 1911.
(42) Fujita, H.; Fujita, T.; Sakurai, T.; Yamase, T.; Seto, Y. *Tohoku J. Exp. Med.* **1992**, *168*, 421.
(43) Compain, J. D.; Mialane, P.; Marrot, J.; Sécheresse, F.; Zhu, W.; Oldfield, E.; Dolbecq, A. *Chem.—Eur. J.* **2010**, *16*, 13741.
(44) Liu, X.; Wang, S.; Feng, C. *Chin. J. Chem.* **2010**, *28*, 2411.
(45) Ankur, B.; Lefebvre, F.; Halligudi, S. B. *J. Catal.* **2007**, *247*, 166.
(46) Niu, J. Y.; Chen, G.; Zhao, J. W.; Ma, P. T.; Li, S. Z.; Wang, J. P.; Li, M. X.; Bai, Y.; Ji, B. S. *Chem.—Eur. J.* **2010**, *16*, 7082.
(47) Xue, S.; Chai, A.; Cai, Z.; Wei, Y.; Xiang, C.; Bian, W.; Shen, J. *Dalton Trans.* **2008**, 4770.
(48) Jasmin, C.; Raybaud, N.; Chermann, J. C.; Haapala, D.; Sinoussi, F.; Loustau, C. B.; Bonissol, C.; Kona, P.; Raynaud, M. *Biomedicine* **1973**, *18*, 319.
(49) Liu, Y.; Tian, S.; Liu, S.; Wang, E. *Transition Met. Chem.* **2005**, *30*, 113.
(50) Si, Y.; Chen, W.; Zhang, Z.; Wang, E. *J. Theor. Comput. Chem.* **2009**, *08*, 773.
(51) Laurencin, D.; Villanneau, R.; Gérard, H.; Proust, A. *J. Phys. Chem.* **2006**, *110*, 6345.
(52) Hasenknopf, B.; Micoine, K.; Lacôte, E.; Thorimbert, S.; Malacria, M.; Thouvenot, R. *Eur. J. Inorg. Chem.* **2008**, 5001.
(53) Fang, X.; Anderson, T. M.; Hill, C. L. *Angew. Chem., Int. Ed.* **2005**, *44*, 3540.
(54) Bassil, B. S.; Mal, S. S.; Dickman, M. H.; Kortz, U.; Oelrich, H.; Walder, L. *J. Am. Chem. Soc.* **2008**, *130*, 6696.
(55) Kikukawa, Y.; Yamaguchi, K.; Mizuno, N. *Angew. Chem., Int. Ed.* **2010**, *49*, 6096.
(56) Sadler, P. J.; Li, H.; Sun, H. *Coord. Chem. Rev.* **1999**, *185−186*, 689.
(57) Kirschner, S.; Wei, Y. K.; Francis, D.; Bergman, J. *J. Med. Chem.* **1966**, *9*, 369.
(58) Skinner, S. M.; Swatzell, J. M.; Lewis, R. W. *Res. Commun. Chem. Pathol. Pharmacol.* **1978**, *19*, 165.
(59) Köpf-Maier, P.; Klapötke, T. *Inorg. Chim. Acta* **1988**, *152*, 49.
(60) Li, M. X.; Yang, M.; Niu, J. Y.; Zhang, L. Z.; Xie, S. Q. *Inorg. Chem.* **2012**, *51*, 12521.
(61) Li, M. X.; Lu, Y. L.; Yang, M.; Li, Y.; Zhang, L. Z.; Xie, S. Q. *Dalton Trans.* **2012**, *41*, 12882.
(62) Li, M. X.; Zhang, L. Z.; Yang, M.; Niu, J. Y.; Zhou, J. *Bioorg. Med. Chem. Lett.* **2012**, *22*, 2418.
(63) Zhang, L. Z.; An, G. Y.; Yang, M.; Li, M. X.; Zhu, X. F. *Inorg. Chem. Commun.* **2012**, *20*, 37.
(64) Lu, W. G.; Gu, J. Z.; Jiang, L.; Tan, M. Y.; Lu, T. B. *Cryst. Growth Des.* **2007**, *8*, 192.
(65) Ramla, M. M.; Omar, M. A.; Tokuda, H.; El-Diwani, H. I. *Bioorg. Med. Chem.* **2007**, *15*, 6489.
(66) Sheldrick, G. M. *SHELXL 97 Program for Crystal Structure Refinement*; University of Göttingen: Göttingen, Germany, 1997.
(67) Sheldrick, G. M. *SHELXL 97 Program for Crystal Structure Solution*; University of Göttingen: Göttingen, Germany, 1997.
(68) Liu, J. R.; Chen, B. Q.; Yang, B. F.; Dong, H. W.; Sun, C. H.; Wang, Q.; Song, G.; Song, Y. Q. *World J. Gastroenterol.* **2004**, *10*, 348.
(69) Liu, Q.; Dong, H. W.; Sun, W. G.; Liu, M.; Ibla, J. C.; Liu, L. X.; Parry, J. W.; Han, X. H.; Li, M. S.; Liu, J. R. *Arch. Toxicol.* **2013**, *87*, 481.
(70) Liu, J. R.; Li, B. X.; Chen, B. Q.; Han, X. H.; Xue, Y. B.; Yang, Y. M.; Zheng, Y. M.; Liu, R. H. *World J. Gastroenterol.* **2002**, *8*, 224.
(71) Bi, L. H.; Al-Kadamany, G.; Chubarova, E. V.; Dickman, M. H.; Chen, L. F.; Gopala, D. S.; Richards, R. M.; Keita, B.; Nadjo, L.; Jaensch, H.; Mathys, G.; Kortz, U. *Inorg. Chem.* **2009**, *48*, 10068.
(72) Brown, D.; Altermatt, D. *Acta Crystallogr., Sect. B* **1985**, *41*, 244.
(73) Fu, N.; Lu, G. X. *Chem. Commun.* **2009**, 3591.
(74) Bösing, M.; Nöh, A.; Loose, I.; Krebs, B. *J. Am. Chem. Soc.* **1998**, *120*, 7252.
(75) Tian, A. X.; Ying, J.; Peng, J.; Sha, J. Q.; Pang, H. J.; Zhang, P. P.; Chen, Y.; Zhu, M.; Su, Z. M. *Inorg. Chem.* **2008**, *48*, 100.
(76) Thompson, C. B. *Science* **1995**, *267*, 1456.
(77) Vaux, D. L.; Korsmeyer, S. J. *Cell* **1999**, *96*, 245.
(78) Hengartner, M. O. *Nature* **2000**, *407*, 770.
(79) Danial, N. N.; Korsmeyer, S. J. *Cell* **2004**, *116*, 205.
(80) Ansari, N.; Khodagholi, F.; Amini, M. *Eur. J. Pharmacol.* **2011**, *658*, 84.
(81) Fan, X. Q.; Guo, Y. J. *Cell Res.* **2001**, *11*, 1.
(82) Aguirre, A.; Gonzalez, A.; Planell, J. A.; Engel, E. *Biochem. Biophys. Res. Commun.* **2010**, *393*, 156.
(83) Bremer, E.; van Dam, G.; Kroesen, B. J.; de Leij, L.; Helfrich, W. *Trends Mol. Med.* **2006**, *12*, 382.
(84) Mahmood, Z.; Shukla, Y. *Exp. Cell. Res.* **2010**, *316*, 887.
(85) Lebedeva, I.; Rando, R.; Ojwang, J.; Cossum, P.; Stein, C. A. *Cancer Res.* **2000**, *60*, 6052.
(86) Rege, Y. D.; Rangnekar, V. M. *Curr. Pharm. Des.* **2004**, *10*, 523.
(87) Oltersdorf, T.; Elmore, S. W.; Shoemaker, A. R.; Armstrong, R. C.; Augeri, D. J.; Belli, B. A.; Bruncko, M.; Deckwerth, T. L.; Dinges, J.; Hajduk, P. J.; Joseph, M. K.; Kitada, S.; Korsmeyer, S. J.; Kunzer, A. R.; Letai, A.; Li, C.; Mitten, M. J.; Nettesheim, D. G.; Ng, S.; Nimmer, P. M.; O'Connor, J. M.; Oleksijew, A.; Petros, A. M.; Reed, J. C.; Shen, W.; Tahir, S. K.; Thompson, C. B.; Tomaselli, K. J.; Wang, B.; Wendt, M. D.; Zhang, H.; Fesik, S. W.; Rosenberg, S. H. *Nature* **2005**, *435*, 677.
(88) Zhou, C.; Mao, X. P.; Guo, Q.; Zeng, F. Q. *Clin. Exp. Dermatol.* **2009**, *34*, e537.
(89) Xue, H. Y.; Niu, D. Y.; Gao, G. Z.; Lin, Q. Y.; Jin, L. J.; Xu, Y. P. *Mol. Biol. Rep.* **2011**, *38*, 3561.
(90) Tooze, S. A.; Codogno, P. *EMBO J.* **2011**, *30*, 1185.
(91) Kluck, R. M.; Bossy-Wetzel, E.; Green, D. R.; Newmeyer, D. D. *Science* **1997**, *275*, 1132.
(92) Yang, J.; Liu, X.; Bhalla, K.; Kim, C. N.; Ibrado, A. M.; Cai, J.; Peng, T. I.; Jones, D. P.; Wang, X. *Science* **1997**, *275*, 1129.
(93) Tsuchiya, Y.; Yamashita, S. *J. Biol. Chem.* **2011**, *286*, 15806.
(94) Mayo, M. W.; Baldwin, A. S. *Biochim. Biophys. Acta* **2000**, *1470*, M55.
(95) Campbell, K. J.; Rocha, S.; Perkins, N. D. *Mol. Cell* **2004**, *13*, 853.
(96) Yu, L. L.; Yu, H. G.; Yu, J. P.; Luo, H. S.; Xu, X. M.; Li, J. H. *World J. Gastroenterol.* **2004**, *10*, 3255.
(97) Morotti, A.; Parvis, G.; Cilloni, D.; Familiari, U.; Pautasso, M.; Bosa, M.; Messa, F.; Arruga, F.; Defilippi, I.; Catalano, R.; Rosso, V.; Carturan, S.; Bracco, E.; Guerrasio, A.; Saglio, G. *Leukemia* **2007**, *21*, 1305.
(98) Cianciulli, A.; Acquafredda, A.; Cavallo, P.; Saponaro, C.; Calvello, R.; Mitolo, V.; Panaro, M. A. *Immunopharmacol. Immunotoxicol.* **2009**, *31*, 51.

(99) Orlowski, R. Z.; Baldwin, A. S., Jr. *Trends Mol. Med.* **2002**, *8*, 385.
(100) Lin, A.; Karin, M. *Semin. Cancer Biol.* **2003**, *13*, 107.